Electrochemical reduction of CO_2 to ethylene with 32% lower energy at 80% lower cost via coproduction of glycolic acid

M.A. Khan[1*], Shariful Kibria Nabil[1*], Tareq A. Al-Attas[1], Soumyabrata Roy[2], M.M. Rahman[2], Stephen Larter,[3] Pulickel M. Ajayan[2], Jinguang Hu[1+], and Md Golam Kibria[1+]

[*]Equal contribution

[1]Department of Chemical and Petroleum Engineering, University of Calgary, 2500 University Drive, NW, Calgary, Alberta T2N 1N4, Canada.

[2]Department of Materials Science and NanoEngineering, Rice University, 6100 Main St., Houston, TX 77030, USA.

[3]Department of Geosciences, University of Calgary, 2500 University Drive, NW, Calgary, Alberta T2N 1N4, Canada.

Abstract

We are in a race against time to implement technologies for carbon capture, conversion, and utilization (CCU) to create a closed anthropogenic carbon cycle. Renewable energy powered electrochemical CO_2 reduction (eCO_2R) to fuels and chemicals is an attractive technology in this context. Here, we demonstrate a strategy to drive economic feasibility of eCO_2R to ethylene (C_2H_4), the largest produced organic chemical, by coupling with glycerol oxidation on anode. Our gold nano-dendrite anode catalyst demonstrated very high activity (J ~377 mA/cm^2 at 1.2 V vs reversible hydrogen electrode) and selectivity (~50% to glycolic acid (GA)) for glycerol oxidation. The co-electrolysis process demonstrated record high selectivity of ~60% for C_2H_4 production at a very low cell voltage of ~ 1.7 V, translating to 32% reduction in required energy compared to conventional eCO_2R with water oxidation reaction on anode. The experimental results were complemented with a detailed technoeconomic analysis that indicated economic feasibility will depend on several factors such as price of organic feed, selectivity of anode electrode, market value of chemicals produced and most importantly cost of separation and purification. Our results indicate that C_2H_4 produced via conventional eCO_2R would require electricity price to plummet to <1 cents/kWh to be cost-competitive, while a co-electrolysis process to produce C_2H_4 and GA will help reduce C_2H_4 production cost by ~ 80% to ~1.08 $/kg, reaching cost parity at electricity price of 5 cents/kWh. This study may trigger research efforts for design of electrochemical processes with low electricity requirement using cheap industrial waste streams.

Keywords: CO_2 reduction; ethylene; emissions; glycerol; energy; oxidation; biomass valorization

*Correspondence: md.kibria@ucalgary.ca; jinguang.hu@ucalgary.ca

Introduction

Electrochemical reduction of CO_2 (eCO_2R) to fuels and valuable chemicals has gained traction as a solution to store renewable electricity, reduce net carbon emissions and generate feedstock for chemical industry.[1-3] CO_2 can go through a 2, 4, 6, 8, 12, or even an 18-electron reduction pathway to produce products such as carbon monoxide, methane, ethylene, formic acid, methanol, ethanol, and propanol.[4] The field has seen a marked increase in research activity over the past few years and many products such as CO and formic acid can now be produced at high current density, faradaic efficiency (FE) and energy efficiency (EE).[5-8] The question arises: What are the near-term target products to achieve market and cost competitiveness? Obviously, this is dictated by market demand and growth of the product of interest as well as the technology readiness level (TRL). This is a question that has recently been addressed by several technoeconomic analysis and perspective reports.[4,9-11] The wide consensus is that based on current economic conditions and catalyst performance, products requiring two electron transfer, such as CO and formic acid, would be profitable and feasible in near-term.[4,12] This is because these products offer highest value per electron and thus reap the economic benefits of low power requirement, which reduces electrolyzer size (capital costs) and electricity use (operating costs).[4] However, today's small market (0.6 Mtons/year global production) of formic acid and the difficulty associated with storing and transporting CO warrant the need to look at alternatives.[4,12]

Of all eCO_2R products, ethylene (C_2H_4) has the largest market of ~ $230 billion and worldwide production of ~150 Mtons/year, which exceeds that of any organic chemical compound.[12] C_2H_4 is widely used in a range of industries and applications with the largest outlet being the polymer industry for synthesis of the world's most heavily used plastics such as polyethylene (116 Mtons/year), polyvinyl chloride (38 Mtons/year), and polystyrene (25 Mtons/year).[12] The next largest consumer of C_2H_4 is ethylene oxide (EO) which is primarily used to make ethylene glycol, the compound is used to produce antifreeze, detergents, textiles etc. C_2H_4 production from CO_2 could potentially reduce 862 Mtons of CO_2/year; suggesting that ethylene is the most attractive target for meaningful CO_2 emissions reductions.[12,13] In recent years there has been lot of focus on electrochemical conversion of CO_2 to C_2H_4, mostly using Cu based catalysts, with reported FE > 50%.[14-16] The challenge with eCO_2R to C_2H_4 is the 12-electron process, large ΔG^o = 1331.4 kJ/mol. Based on a cathodic and anodic overpotential of 0.6 V and FE_{C2H4} of ~90%, an electricity requirement of ~ 22.3 kWh/kg_{C2H4} can be calculated.[13] This results in highest capital

and operating costs/kg of C_2H_4 versus other products.[4,12] These high costs, along with a large CO_2 feedstock requirement (3.14 $kgCO_2/kgC_2H_4$), impedes the eCO_2-to-C_2H_4 pathways to be cost competitive with current market price (US $1000-1300/ton C_2H_4).[4,10,12]

Recently, there have been growing interest in replacing the anodic half of the eCO_2R reaction i.e., oxygen evolution reaction (OER) by oxidation of cheap and abundant organic materials to decrease required overpotential.[17,18] In this context, glycerol is of interest as it is a cheap byproduct of biodiesel and soap manufacturing and is produced at industrial scales (4.3 Mtons/year) with 80% purity at a low cost of about US $200/ton.[18] Thermodynamic data indicates that the use of glycerol as anodic reactant in an electrolysis cell could be more energetically favorable over OER. This is due to lower theoretical cell voltage for glycerol electrolysis (U^0_{cell} = 0.003 V, n = 14 for the complete oxidation of glycerol into CO_2) compared to water electrolysis (U^0_{cell} = +1.229 V, n = 2), where n is the number of electrons generated per molecule oxidized.[19] However, complete oxidation of glycerol to CO_2 impedes environmental and economic prospects and the overall process will only be viable if one can achieve partial oxidation to selectively produce valuable chemicals. Recent reports on co-electrolysis of CO_2 and glycerol demonstrated its potential to reduce overall electricity consumption, however the reported C_2H_4 selectivity was low at ~ 23% without analysis of the oxidation products.[18] Moreover, there are no reports on the technoeconomic feasibility of such a process to identify feasible glycerol oxidation products and establish electrolyzer performance targets.

In this study, we report co-electrolysis process, with eCO_2R to C_2H_4 on Cu cathode coupled with glycerol oxidation reaction (GOR) on Au nano-dendrite anode (Au-ND) to selectively make valuable chemicals. Our Au-ND anode catalyst demonstrated record high activity (J ~377 mA/cm^2 at 1.2 V vs RHE) and selectivity (~50% to glycolic acid) for glycerol oxidation. The co-electrolysis experiments were carried out in a zero gap electrolyzer which helped us achieve high FE of ~60% to C_2H_4, and upon addition of glycerol to anolyte feed we were able to reduce the required voltage for reaction by ~ 0.8 V that translates to a reduction in required electricity by ~ 32%. Lastly, we carry out a detailed technoeconomic analysis (TEA) of an electrochemical process to produce C_2H_4 via eCO_2R and formic acid (FA)/glycolic acid (GA) via GOR. Our results indicate that a co-electrolysis process to produce C_2H_4 and GA will help reduce the production cost of C_2H_4 by ~ 80%. In contrast, FA is not a suitable target as the market price is not enough to offset the cost of separation and glycerol feed.

1. Results and discussion

Fig. 1(a) shows the cyclic voltammetry (CV) curves of Au nano-dendrites (Au-ND) as well as nickel foam (NiF) with (glycerol concentration of 0.05 M) and without glycerol in 3M KOH electrolyte. The details of catalyst synthesis and electrochemical testing are provided in SI. The electrochemical behavior of nickel in alkaline conditions is well understood where the peak centered at ~1.3 V vs. RHE can be ascribed to the oxidation of β-$Ni(OH)_2$ to β-NiOOH with the onset of the oxygen evolution reaction (OER) at ~1.45 V vs RHE.[20] With the addition of 0.05 M glycerol, a dramatic increase in current is observed with the onset potential at ~1.3 V vs RHE, by virtue of β-NiOOH being the electrochemically active phase towards GOR.[20,21] In contrast, on Au-ND catalyst, GOR begins at much lower potential at ~0.6 V vs RHE, peak current occurs at 1.2 V vs RHE and the increase in current at 1.3 V vs RHE can be assigned to gold oxidation.[22] A detailed assignment of different regions in CV scan of Au-ND catalyst is shown in supplementary Fig S1. In the backward scan, reactivation of catalyst surface causes the formation of the anodic peak at ~1.1 V vs RHE. This peak is primarily related to the removal of intermediate species not completely oxidized in the forward scan.[23,24] The glycerol concentration was optimized for Au-ND catalyst based on current density at 1.2 V vs RHE (Fig. 1(b)), since there is negligible current from gold oxidation or OER at this voltage. Similarly, the glycerol concentration was optimized for NiF, based on current density at 1.5 V vs RHE (Fig. S2). The scans revealed that 0.5 M glycerol concentration was optimum, as higher glycerol concentrations led to rapid drop in current density and deactivation of both catalysts. This can be attributed to the saturation of active sites with glycerol that inhibits the OH^- adsorption and causes decrease in current.[23] The CV curve of Au-ND catalyst at 0.5 M glycerol concentration (Fig. 1(c)) revealed a maximum current density of ~377 mA/cm^2 for GOR at 1.2 V vs RHE which represents a significant improvement from reported current densities in alkaline conditions (Fig. 1(d)). The references for Fig. 1(d) are tabulated in supplementary information (Table S1). We also observed the disappearance of anodic peak in the backward scan which could possibly be due to removal of the intermediate species in forward scan, owing to the higher current densities.

The high activity achieved is due to combination of the strong base (3M KOH), and use of stable and high surface area catalyst. In alkaline media, the kinetics of alcohol electro-oxidation is faster than in acidic ones, as the base catalyzes the first deprotonation step for the electro-oxidation of alcohols to form alkoxide species, while the second deprotonation step depends on

the catalyst.[25] The trade-off of working in alkaline conditions is the limited choice of catalyst for GOR. While Pt and Pd based catalysts have the lower overpotential for GOR than Au, they suffer from low current density and stability due to formation of surface poisoning oxides in alkaline conditions.[19,23,26] In contrast, Au and Ni are less prone to poisoning by adsorbed species such as CO, which improves the activity and stability for GOR as also observed in earlier reports.[19,27] As a comparison, the electrochemical results of Pt/NiF for GOR is presented in the SI (Fig. S3), which showed much lower stability versus Au-ND catalysts.

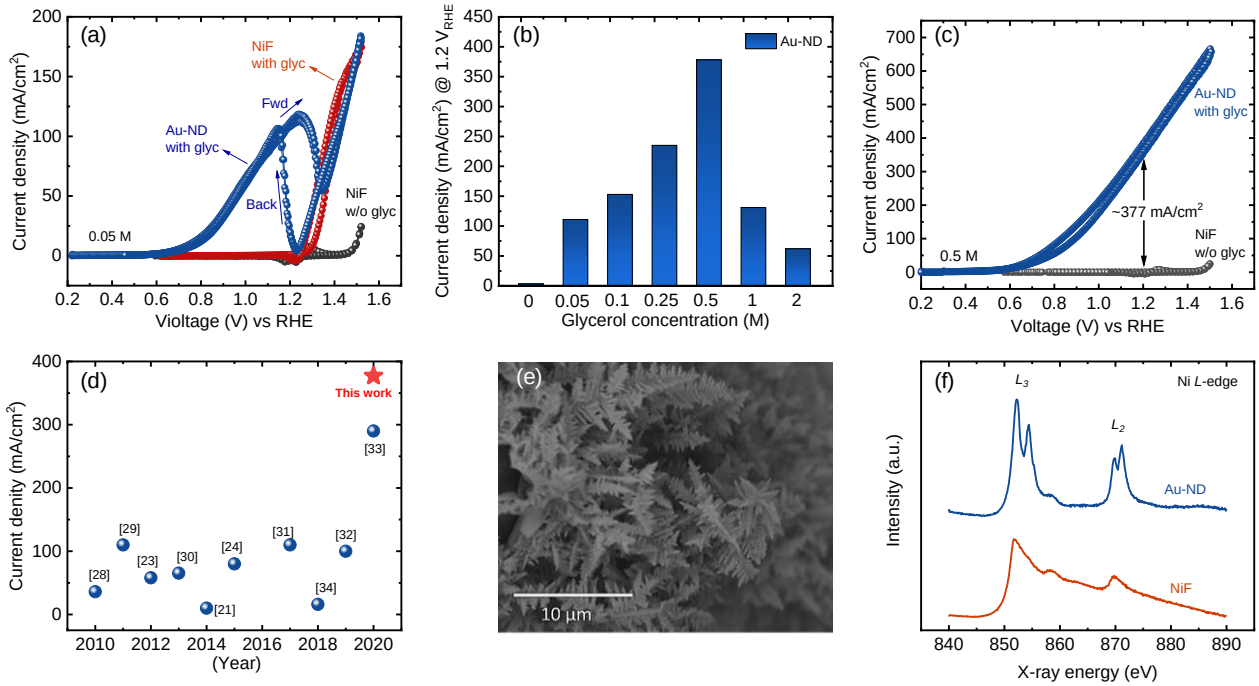

Figure 1. (a) CV curves for Au-ND and NiF catalysts for GOR in 3 M KOH at a glycerol concentration of 0.05 M. (b) Current density at 1.2 V vs RHE for Au-ND catalyst as a function of glycerol concentration. (c) CV curves for Au-ND catalysts for GOR in 3 M KOH at a glycerol concentration of 0.5 M. (d) Highest peak current densities reported in literature for GOR in alkaline conditions at ≤ 1.5 V vs RHE. References are tabulated in Table S1 of SI.[21,23,24,28-34] (e) SEM images showing presence of Au-ND structures. (f) Ni L-edge soft XAS spectra for on Au-ND and NiF catalysts.

The high electrochemical current achieved for GOR is also a function of high surface area Au-ND structures (Fig. 1(e), S4), formed due to galvanic replacement (GR) process used for synthesis. The GR process is a redox reaction between two metals where the lesser noble metal (Ni) has the tendency to reduce the more noble metal (Au) cation having a higher redox potential

without application of an external current and generally leads to nanomaterials displaying a high surface to volume ratio and large pore volumes.[35,36] In the case of Au and Ni, the following galvanic replacement reaction is expected to occur spontaneously in aqueous solution:[35]

$$3Ni^{0}_{(s)} + 2Au^{3+}_{(aq.)} \rightarrow 2Au^{0}_{(s)} + 3Ni^{2+}_{(aq.)}$$

To confirm the galvanic replacement process, we measured soft X-ray absorption spectroscopy (XAS) on the Ni $L_{2,3}$-edges. Metal L-edge XAS is a powerful probe of the local electronic structure that is sensitive to the valency, spin, and symmetry of the metal atom. The main features in the spectrum (Fig. 1(f)) are the two maxima at 852.6 and 870 eV corresponding to edges L_3 ($2p_{3/2} \rightarrow 3d$, ~853 eV) and L_2 ($2p_{1/2} \rightarrow 3d$, ~870 eV) and a small peak at ~859 eV called the satellite feature (due to the ligand orbitals mixing with the Ni orbitals).[37,38] The fine splitting in both L_3 and L_2 is due to the crystal feld effect and are sensitive to the electronic and oxidation state of the metal, and to the local geometry. Based on previous Ni L-edge XAS studies of nickel oxides, intensity ratio of the double-peak features in the Ni L_3 region fingerprints the oxidation state of the Ni atoms in the catalyst.[37,39] From the overall shape of the L_3 edge, it is evident that fresh NiF is composed of metallic nickel.[37] In contrast, Au-ND sample shows increased intensity of peak at 855 eV indicating the presence of Ni^{2+}.

To gain more information about surface electronic state and chemical composition, the surface was characterized using X-ray photoelectron spectroscopy (XPS). XPS spectra for Au4f, Ni2p and O1s are presented in supplementary Fig. S6. The presence of metallic gold is seen by the peaks centered at 84.1 and 87.7 eV. The peak positions, spin–orbit splitting (SOS) of 3.6 eV and full width at half maximum (FWHM) ($Au4f_{7/2}$ = 0.7 eV; $Au4f_{5/2}$ = 0.7) are characteristic of metallic gold. For the Ni2p spectra, the peak at 852.71 eV with a FWHM of 1.2 eV is characteristic of Ni^0. The contribution of this metallic Ni peak decreases in the Au-ND catalyst versus NiF catalyst, again indicative of the galvanic replacement process. The same behavior has earlier been observed with XPS for Au/Ni samples, indicating a suppression of Ni^0 peak along with the development of a more pronounced NiO peak, while Au was present in its metallic form.[40]

After optimization of catalysts and conditions for GOR, the co-electrolysis experiments were carried out in a zero-gap membrane electrode assembly (MEA). Of late, MEA setup has been the preferred choice for CO_2 electrolysis due to the inherent carbonate formation and catalyst poisoning in alkaline flow cells as described in recent reports.[15,41,42] A schematic of the MEA setup is shown in Fig. 2(a) where we used 3 M KOH with (0.5 M glycerol) and without glycerol as

anolyte. A 250 nm thick sputtered copper on polytetrafluoroethylene (PTFE) gas diffusion layer (GDL) was used as cathode. Our previous work demonstrates that sputtered Cu on PTFE based GDL enables high stability and selectivity.[14] Further details on the MEA setup are available in the supplementary. Fig. 2(b) shows the current-voltage behavior of the CO_2 electrolyzer with (0.5 M glycerol) and without glycerol using NiF and Au-ND catalysts. With the addition of glycerol in the anode feed, there is a significant reduction of ~0.85 V in onset potential for the reaction, with significantly higher current densities at any given voltage.

Product analysis of the cathode outlet gas stream using gas chromatography (GC), indicated C_2H_4 as the major product with H_2 as major by-product and small amounts of CO, like previous reports for Cu-based catalysts (See supplementary Fig. S7 for detailed product quantification).[14-16] Fig. 2(c) summarizes the electrochemical performance of co-electrolysis experiments. When using 3 M KOH as anolyte feed, we achieved high FE_{C2H4} of ~60% at voltages in the range of 2.5-2.7, which is on par with the best reports on eCO_2R to C_2H_4.[14,15] Upon addition of 0.5 M glycerol to the anolyte feed, the required voltage to reach the same current density and FE_{C2H4} decreased by 0.4 V to 2.1-2.3 V. Replacing the NiF anode with Au-ND further reduced the required voltage by 0.4 V to 1.7-1.9 V, without compromising current density or FE_{C2H4}, suggesting that anode catalyst and anolyte do not affect the selectivity of cathode electrode. Thus, we were able to reduce ~ 0.8 V or 32% required electricity using co-electrolysis approach versus conventional CO_2R while maintaining record high (60%) selectivity towards C_2H_4. At higher current densities, the competing hydrogen evolution reaction (HER) was more dominant. This could be optimized by reconstructing the surface of sputtered copper using carbon or other surface treatment methods, as we have demonstrated in earlier reports.[10,16,43,44] Fig. 2(d) summarizes the FE_{C2H4} reported in literature from CO_2 electrolysis, suggesting that high FE has generally been reported at > 2.5 V, while our co-electrolysis experiments show similar FE_{C2H4} (60%) at a much lower voltage (1.7 V).

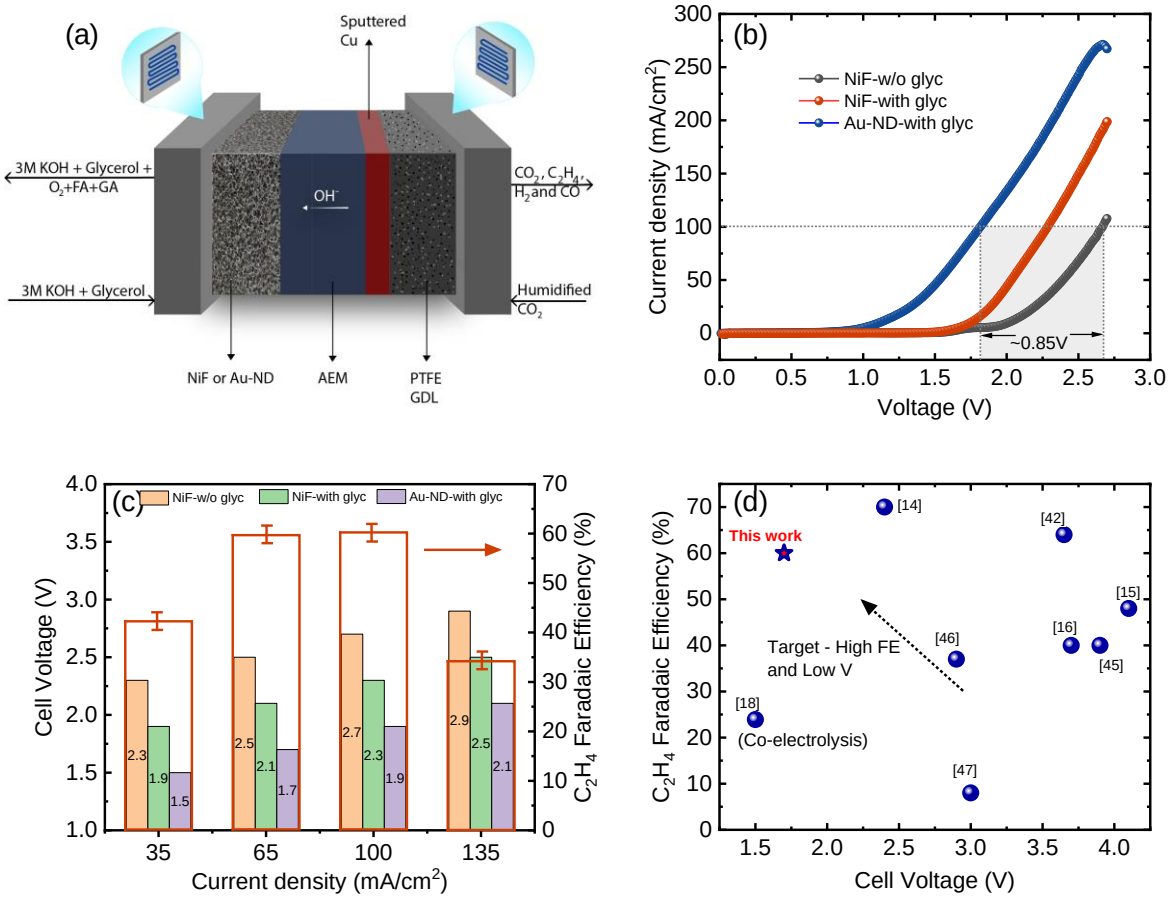

Figure 2. (a) Schematic of MEA setup used for co-electrolysis experiments with eCO_2R on cathode and GOR on anode. (b) LSV curves for co-electrolysis using different anode electrodes with (0.5 M) and w/o glycerol in anolyte. (c) Cell voltage (left y-axis) and FE_{C2H4} (right y-axis) as function of current density when using different anode electrodes. All experiments were run under identical conditions i.e., sputtered copper as cathode and 3 M KOH + 0.5 M glycerol as anolyte. (d) Reported C_2H_4 FE as function of full cell voltage for electrochemical CO_2R. References are tabulated in Table S2 of SI.[14-16,18,42,45-47]

The anodic products formed during the co-electrolysis experiments of Fig. 2, were determined by ^1H NMR as shown in Fig. 3(a). The CO_2 electrolyzer was run at a constant current ~ 65 mA/cm^2 using 0.5 M glycerol in 3 M KOH as anode feed and displayed good stability for more than 4 hours (Fig. S8). In all reactions in alkaline conditions, the products were obtained as salts, but they were marked as the acid forms for simplicity and comparison. The NMR results indicated the presence FA and GA when using the NiF electrode while the Au-ND electrode showed presence of FA, GA and glyceric acid (GLY). Quantification of the products (Fig. 3(b)),

revealed that the NiF is highly selective to FA while Au is more selective to GA. This has been observed in earlier reports as well where Au was shown to be more selective to GA compared to Pd catalysts.[25,48] GOR on gold surfaces has been well studied whereby glycerol is first oxidized to glyceraldehyde (GLAD) by the coordination of the catalyst and base.[49] In this step, glycerol is first deprotonated (H_α in the R-CHH_β-OH_α) which is catalyzed by base, followed by the second deprotonation depending on the ability of the catalyst to abstract the H_β.[49] The resulting GLAD further undergoes a metal-catalyzed oxidation reaction to GLY but in the case of the Au, GLAD production is not observed, because of the low overpotential on gold, which makes GLAD an unstable intermediate.[49] As a next step, GLY is further oxidized via C-C cleavage to products such as GA, FA or Oxalic Acid. The selective oxidation of glycerol via an electrochemical process is very attractive due to simplicity of reactor, and mild operating condition, which has the potential to decrease the operating costs compared to those of conventional routes.

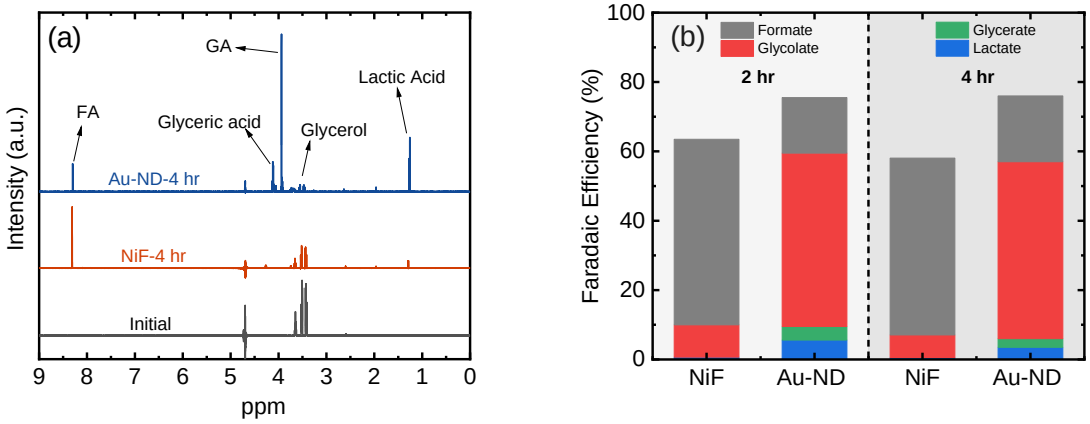

Figure 3. (a) ^{1}H NMR spectra of products before and after 4 h anodic glycerol oxidation on NiF and Au-ND electrode. The experiments were conducted at constant current ~ 65 mA/cm^2 using 0.5 M glycerol in 3 M KOH as anode feed. Dimethyl sulfoxide (DMSO) was used as the internal standard. (b) Product distributions from anolyte feed during co-electrolysis experiments upon using different anode electrodes: NiF and Au-ND.

To gain a better understanding of the consequences and feasibility of co-electrolysis process, we carried out a detailed techno-economic analysis (TEA) based on the performance achieved in our experiments. While there are several TEA studies for electrochemical reduction of CO_2, none of them analyse a process replacing the anodic OER.[4,10] For a co-electrolysis process, it is

important to analyse the effect of feed price and cost of separation of anodic products on the process economics. Fig. 4. shows the schematic of a co-electrolysis process in which concentrated CO_2 stream is fed along with water + glycerol mixture to the CO_2 electrolyzer, where liquid and gas products are formed. The electrolyzer operating conditions in the model was taken from the experimental results as discussed in Figure 2, i.e., current density of ~ 100 mA/cm^2, voltage between 1.9-2.7 V depending on the anodic reaction, FE_{C2H4} ~60% and $FE_{GA/FA}$ ~50%. Since long term catalyst stability is yet to be tested, it was assumed on the lower end at 1 year for all cases. The liquid products are fed to a separation system (distillation) to extract the liquid products, while the electrolyte is recycled back to the electrolyzer. The gas products, along with unconverted CO_2 and by-product hydrogen, are separated in a gas separation unit, from which the CO_2 is recycled back to the reactor.

To provide an estimate for the capital costs of an alkaline CO_2 electrolyzer system, an alkaline water electrolyzer stack with a cost of $450/kW was used as a representative model.[50,51] The auxiliary systems that is the balance of plant (BoP) was also taken at $450/kW and represents ~ 50% of electrolyser system (stack+BoP) cost in an alkaline electrolyser.[50,51] The separation process was modelled using Aspen Plus V10.0, and capital and utility costs were estimated using the Aspen Process Economic Analyzer V10.0. To estimate the return on capital investment for the development of a co-electrolysis facility, a discounted cash flow spreadsheet was developed to estimate the capex, yearly operating costs and revenue over the project lifetime. It was assumed that capex allocation and construction of the plant was completed in the first three years, with plant operation beginning in the fourth year. A standard nominal interest rate (NIR) of 10%, compounded annually, and a total effective income tax rate of 38% was assumed.[4] Further details of the process, financial and reaction parameters used in the analysis are listed in supplementary Tables S3-S5.

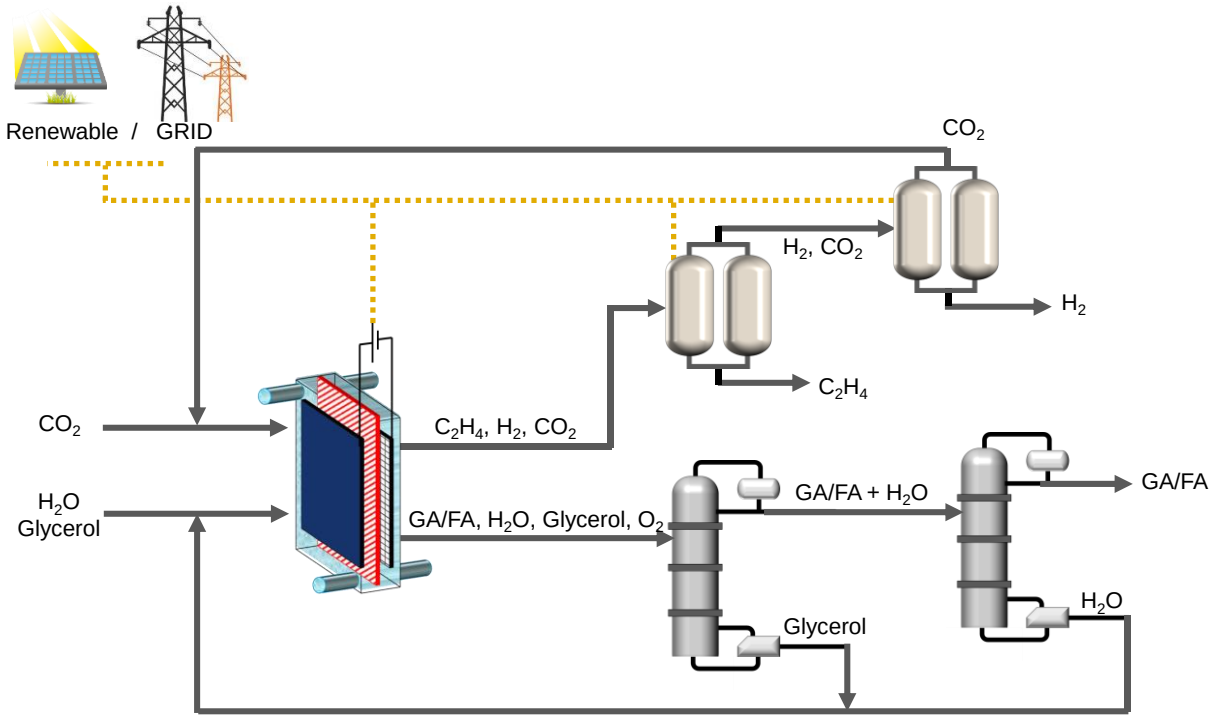

Figure 4. Schematic of co-electrolysis process combining CO_2R and GOR for coproduction of C_2H_4, H_2 and GA/FA.

Fig. 5(a) shows the sensitivity analysis of the base case scenario where CO_2R-to-C_2H_4 is coupled with OER on anode, and each parameter was varied by ± 50%. We estimated the minimum selling price (MSP) of C_2H_4 (MSP_{C2H4}) is ~ 5.2 $/kg which is almost three times higher than current market price (MP) of ~ 1.0-1.3 $/kg.[10,12] It is important to note that as H_2 compression and storage was not modelled in the study, the H_2/O_2 produced were not considered as revenue streams. Among all parameters, FE_{C2H4}, voltage, and electricity price have the biggest effect on the MSP. These observations are in line with previous reports and is attributed to the 12-electron process, leading to high capital and operating costs as shown in the supplementary Fig. S9-11.[4,10,12] Upon addition of glycerol (250 $/ton) to the anode feed, in conjunction with the separation unit for anode products leads to some very interesting observations. The analysis was done for both cases observed in our experiments (Fig 2-3) i.e., FA and GA production, with ~0.4 V and ~0.8 V reduction in voltage respectively, without compromising on FE_{C2H4} and current density. It is important to note that we also assume that the addition of glycerol does not affect stability of catalysts and membrane versus the base case scenario.

The production of FA (85% purity), at a FE of ~50% and which sells at a market price of ~ 980 $/ton[52], has an adverse effect on the MSP_{C2H4} which increases to ~ 6.6 $/kg. FA and water form a maximum-boiling azeotropic mixture whose boiling point is 107.6 °C at 101.3 kPa, making it difficult to separate using distillation.[53] At the same time, reactive distillation provides an alternative approach for separation of multicomponent azeotropic mixtures.[54] By changing substance properties through chemical reaction with appropriate reactants, thermodynamic limitations like azeotrope formation can be avoided, but still requires significant energy. Therefore, the revenue generated by FA will not be able to compensate for the additional operating cost due to glycerol feed and separation of products. A detailed breakdown of capex and opex in different cases is provided in supplementary Fig S8-10. On the other hand, GA has very high market selling price of ~3000-4000 $/ton[55], which helps decrease the MSP_{C2H4} to ~1.08 $/kg. GA is a valuable chemical for the cosmetic industry, household and industrial cleaning industry and is touted to play a key role in future of bioplastics in the form of Poly (glycolic acid) (PGA) or poly(lactic-co-glycolic acid) (PLGA).[56]

With the effect of voltage reduction being addressed in different cases of FA and GA production, we moved to analyze the effect of two other important parameters i.e., FE_{C2H4} and electricity price. Fig. 5(b) shows a contour plot for the base case i.e., OER on anode which indicates that it will be very difficult to make an economically feasible process for CO_2R to C_2H_4 coupled with OER. Even at very low electricity prices of ~ 0.01 $/kWh along with high FE_{C2H4} > 70%, conventional eCO_2R will find it difficult to bring the MSP_{C2H4} down to current market price. It will need several factors such as electrolyzer performance (current + voltage + selectivity + stability), capex costs, electricity price, to fall into place together for the process to be economically competitive. For co-electrolysis setups, the economic feasibility depends on several factors such as cost of organic feed, selectivity to make valuable chemicals on anode, market value of those chemicals and cost of separation and purification. For the case of anodic GOR to FA (Fig. 5(c)), the process will not make economic sense at any electricity price or FE_{C2H4}. In contrast if one can make valuable products such as GA at high selectivity (Fig. 5(d)), this could make the eCO_2R to C_2H_4 economically feasible even with an electricity price of ~0.05 $/kWh. Further reduction in electricity price or improvements in FE_{C2H4} could lead to significant reduction in C_2H_4 cost, making the process very profitable.

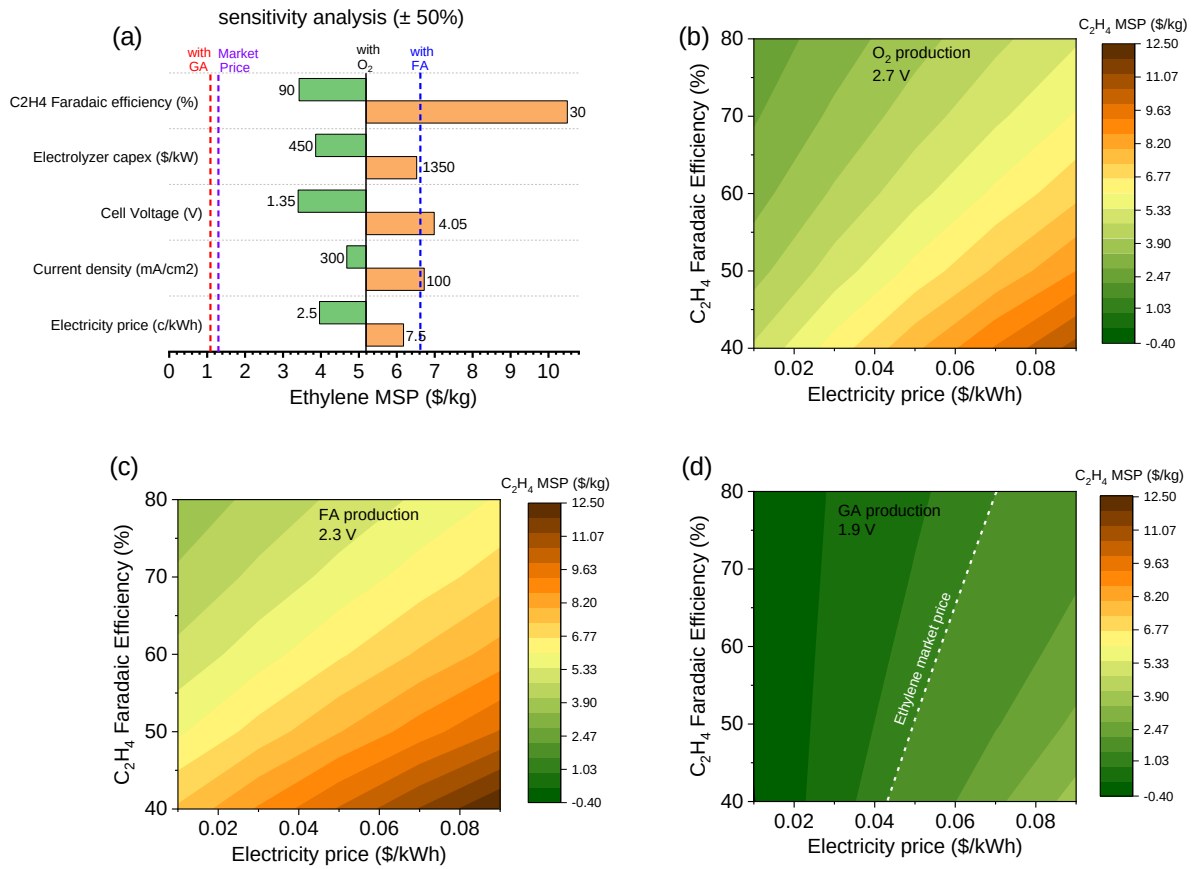

Figure 5. (a) Sensitivity analysis to illustrate the impact of ±50% changes in key parameters for the co-electrolysis process. The dash lines indicate market price (purple), calculated MSP_{C2H4} with FA (blue) or GA (red) as anodic product. Contour plots of FE_{C2H4} versus electricity price for eCO_2 to C_2H_4 coupled with different anodic reactions: (b) OER to produce O_2 (c) GOR to produce FA and (d) GOR to produce GA. Red dash lines indicate current market price of C_2H_4 at 1.3 $/kg.

2. Conclusion and perspective

In summary, we demonstrated the replacement of anodic water oxidation with glycerol oxidation as a strategy to drive economic feasibility for CO_2R to C_2H_4, a reaction which requires significant energy. In the process we synthesized highly active Au-ND catalysts for GOR which demonstrated high current densities and low overpotential. The co-electrolysis experiments with Au-ND as anode for GOR and sputtered copper as cathode for CO_2R helped us achieve high FE of ~60% to C_2H_4, with ~ 0.8 V reduction in voltage, translating to ~32% reduction in required electricity. In addition, we have an added benefit of producing GA at anode with high FE > 50%. Lastly, we carry out a detailed TEA of co-electrolysis process to produce ethylene via CO_2R and

GA/FA via GOR. Our analysis indicated that the economic feasibility depends on several factors such as cost of organic feed, selectivity to make valuable chemicals on anode, market value of those chemicals and most importantly cost of separation and purification. Our results indicate that while a co-electrolysis process to produce C_2H_4 and GA will help reduce the MSP_{C2H4} by ~ 80% to ~1.08 $/kg which is below market price.

While the results presented in this study are a step forward for eCO_2R, it is important to present a perspective on other key aspects. While glycerol could be a promising feedstock, many other organic reactions could be and should be explored to replace OER on anode. Many factors such as the cost of organic material, its scale of production, value and demand of products formed will have to be considered for practical application. There is a lot of scope for researchers to contribute into development of electrocatalysts, membranes and systems for co-electrolysis processes where anodic organic reactions are coupled with H_2 production or CO_2R on cathode. In this context, we believe development of catalysts for electrocatalytic oxidation of a renewable feedstock such as raw biomass with high activity (current density), selectivity and stability could be a breakthrough.

Acknowledgement

The author(s) would like to acknowledge the financial support provided by Canada First Research Excellence Fund (CFREF) at University of Calgary. Part of the research described in this paper was performed at the Canadian Light Source, a national research facility of the University of Saskatchewan, which is supported by the Canada Foundation for Innovation (CFI), the Natural Sciences and Engineering Research Council (NSERC), the National Research Council (NRC), the Canadian Institutes of Health Research (CIHR), the Government of Saskatchewan, and the University of Saskatchewan.

References

1. Adnan, M. A. & Kibria, M. G. Comparative techno-economic and life-cycle assessment of power-to-methanol synthesis pathways. *Appl. Energy.* **278**, 115614 (2020).
2. Nitopi, S. *et al.* Progress and perspectives of electrochemical CO_2 reduction on copper in aqueous electrolyte. *Chem. Rev.* **119**, 7610-7672 (2019).
3. Gurudayal *et al.* Efficient solar-driven electrochemical CO_2 reduction to hydrocarbons and oxygenates. *Energy. Environ. Sci.* **10**, 2222-2230, doi:10.1039/C7EE01764B (2017).
4. Jouny, M., Luc, W. & Jiao, F. General techno-economic analysis of CO_2 electrolysis systems. *Ind. Eng. Chem. Res.* **57**, 2165-2177 (2018).
5. Birdja, Y. Y. *et al.* Advances and challenges in understanding the electrocatalytic conversion of carbon dioxide to fuels. *Nat. Energy.* **4**, 732-745 (2019).
6. Edwards, J. P. *et al.* Efficient electrocatalytic conversion of carbon dioxide in a low-resistance pressurized alkaline electrolyzer. *Appl. Energy.* **261**, 114305 (2020).
7. Liu, M. *et al.* Enhanced electrocatalytic CO_2 reduction via field-induced reagent concentration. *Nature* **537**, 382-386 (2016).
8. Xia, C. *et al.* Continuous production of pure liquid fuel solutions via electrocatalytic CO_2 reduction using solid-electrolyte devices. *Nat. Energy.* **4**, 776-785 (2019).
9. Bushuyev, O. S. *et al.* What should we make with CO_2 and how can we make it? *Joule* **2**, 825-832 (2018).
10. Kibria, M. G. *et al.* Electrochemical CO_2 reduction into chemical feedstocks: from mechanistic electrocatalysis models to system design. *Adv. Mater.* **31**, 1807166 (2019).
11. Mohsin, I. *et al.* Economic and Environmental Assessment of Integrated Carbon Capture and Utilization. *Cell Reports Physical Science* **1**, 100104 (2020).
12. De Luna, P. *et al.* What would it take for renewably powered electrosynthesis to displace petrochemical processes? *Science* **364** (2019).
13. Nabil, S., McCoy, S. & Kibria, M. Comparative Life Cycle Assessment of Electrochemical Upgrading of CO_2 to Fuels and Feedstocks. (2020).
14. Dinh, C.-T. *et al.* CO_2 electroreduction to ethylene via hydroxide-mediated copper catalysis at an abrupt interface. *Science* **360**, 783-787 (2018).
15. Gabardo, C. M. *et al.* Continuous carbon dioxide electroreduction to concentrated multi-carbon products using a membrane electrode assembly. *Joule* **3**, 2777-2791 (2019).
16. Wang, Y. *et al.* Catalyst synthesis under CO_2 electroreduction favours faceting and promotes renewable fuels electrosynthesis. *Nat. Catal.* **3**, 98-106 (2020).
17. Houache, M. S. *et al.* Selective Electrooxidation of Glycerol to Formic Acid over Carbon Supported $Ni_{1-x}M_x$ (M= Bi, Pd, and Au) Nanocatalysts and Coelectrolysis of CO_2. *ACS Appl. Energy. Mater.* (2020).
18. Verma, S., Lu, S. & Kenis, P. J. Co-electrolysis of CO_2 and glycerol as a pathway to carbon chemicals with improved technoeconomics due to low electricity consumption. *Nat. Energy.* **4**, 466 (2019).
19. Houache, M. S., Hughes, K. & Baranova, E. A. Study on catalyst selection for electrochemical valorization of glycerol. *Sustain. Energy. Fuels.* **3**, 1892-1915 (2019).
20. Oliveira, V. *et al.* Kinetic investigations of glycerol oxidation reaction on Ni/C. *Electrocatalysis* **6**, 447-454 (2015).
21. Oliveira, V. *et al.* Studies of the reaction products resulted from glycerol electrooxidation on Ni-based materials in alkaline medium. *Electrochim. Acta.* **117**, 255-262 (2014).

22 Hebié, S., Holade, Y., Servat, K., Kokoh, B. K. & Napporn, T. W. Electrochemical reactivity at free and supported gold nanocatalysts surface. *Catalytic Application of Nano-Gold Catalysts, Mishra, NK, Ed., Intech: Rijeka, Croatia*, 101-130 (2016).
23 Habibi, E. & Razmi, H. Glycerol electrooxidation on Pd, Pt and Au nanoparticles supported on carbon ceramic electrode in alkaline media. *Int. J. Hydrog. Energy.* **37**, 16800-16809 (2012).
24 Marshall, A. T., Golovko, V. & Padayachee, D. Influence of gold nanoparticle loading in Au/C on the activity towards electrocatalytic glycerol oxidation. *Electrochim. Acta.* **153**, 370-378 (2015).
25 Kwon, Y., Lai, S. C., Rodriguez, P. & Koper, M. T. Electrocatalytic oxidation of alcohols on gold in alkaline media: base or gold catalysis? *J. Am. Chem. Soc.* **133**, 6914-6917 (2011).
26 Simões, M., Baranton, S. & Coutanceau, C. Electrochemical valorisation of glycerol. *ChemSusChem.* **5**, 2106-2124 (2012).
27 Liu, Y., Yu, W., Raciti, D., Gracias, D. H. & Wang, C. Electrocatalytic Oxidation of Glycerol on Platinum. *J. Phys. Chem. C.* **123**, 426-432, doi:10.1021/acs.jpcc.8b08547 (2019).
28 Simões, M., Baranton, S. & Coutanceau, C. Electro-oxidation of glycerol at Pd based nano-catalysts for an application in alkaline fuel cells for chemicals and energy cogeneration. *Appl. Catal. B.* **93**, 354-362 (2010).
29 Ilie, A., Simoes, M., Baranton, S., Coutanceau, C. & Martemianov, S. Influence of operational parameters and of catalytic materials on electrical performance of direct glycerol solid alkaline membrane fuel cells. *J. Power. Sources.* **196**, 4965-4971 (2011).
30 Marchionni, A. *et al.* Electrooxidation of Ethylene Glycol and Glycerol on Pd-(Ni-Zn)/C Anodes in Direct Alcohol Fuel Cells. *ChemSusChem* **6**, 518-528 (2013).
31 Dai, C. *et al.* Electrochemical production of lactic acid from glycerol oxidation catalyzed by AuPt nanoparticles. *J. Catal.* **356**, 14-21 (2017).
32 Li, Y., Wei, X., Chen, L., Shi, J. & He, M. Nickel-molybdenum nitride nanoplate electrocatalysts for concurrent electrolytic hydrogen and formate productions. *Nat. Commun.* **10**, 1-12 (2019).
33 Boukil, R. *et al.* Enhanced electrocatalytic activity and selectivity of glycerol oxidation triggered by nanoalloyed silver–gold nanocages directly grown on gas diffusion electrodes. *J. Mater. Chem. A.* **8**, 8848-8856 (2020).
34 Houache, M. S., Cossar, E., Ntais, S. & Baranova, E. A. Electrochemical modification of nickel surfaces for efficient glycerol electrooxidation. *J. Power. Sources.* **375**, 310-319 (2018).
35 Huang, J., Han, X., Wang, D., Liu, D. & You, T. Facile synthesis of dendritic gold nanostructures with hyperbranched architectures and their electrocatalytic activity toward ethanol oxidation. *ACS Appl. Mater. Interfaces.* **5**, 9148-9154 (2013).
36 da Silva, A. G., Rodrigues, T. S., Haigh, S. J. & Camargo, P. H. Galvanic replacement reaction: recent developments for engineering metal nanostructures towards catalytic applications. *ChemComm.* **53**, 7135-7148 (2017).
37 Seifarth, O. *et al.* Metallic nickel nanorod arrays embedded into ordered block copolymer templates. *Thin. Solid. Films.* **515**, 6552-6556 (2007).

38 Gu, W., Wang, H. & Wang, K. Nickel L-edge and K-edge X-ray absorption spectroscopy of non-innocent Ni[$S_2C_2(CF_3)_2]_2^n$ series (n=− 2,− 1, 0): direct probe of nickel fractional oxidation state changes. *Dalton. Trans.* **43**, 6406-6413 (2014).
39 Drevon, D. *et al.* Uncovering the role of oxygen in Ni-Fe (O x H y) electrocatalysts using in situ soft x-ray absorption spectroscopy during the oxygen evolution reaction. *Sci. Rep.* **9**, 1-11 (2019).
40 Sabri, Y. M., Ippolito, S. J., Atanacio, A. J., Bansal, V. & Bhargava, S. K. Mercury vapor sensor enhancement by nanostructured gold deposited on nickel surfaces using galvanic replacement reactions. *J. Mater. Chem.* **22**, 21395-21404 (2012).
41 Ren, S. *et al.* Molecular electrocatalysts can mediate fast, selective CO_2 reduction in a flow cell. *Science.* **365**, 367-369 (2019).
42 Li, F. *et al.* Molecular tuning of CO_2-to-ethylene conversion. *Nature* **577**, 509-513 (2020).
43 Garg, S. *et al.* Advances and challenges in electrochemical CO_2 reduction processes: an engineering and design perspective looking beyond new catalyst materials. *J. Mater. Chem. A.* **8**, 1511-1544 (2020).
44 Kibria, M. G. *et al.* A surface reconstruction route to high productivity and selectivity in CO_2 electroreduction toward C_{2+} hydrocarbons. *Adv. Mater.* **30**, 1804867 (2018).
45 De Arquer, F. P. G. *et al.* CO_2 electrolysis to multicarbon products at activities greater than 1 A cm^{-2}. *Science* **367**, 661-666 (2020).
46 Huan, T. N. *et al.* Low-cost high-efficiency system for solar-driven conversion of CO_2 to hydrocarbons. *PNAS.* **116**, 9735-9740 (2019).
47 Lee, J., Lim, J., Roh, C.-W., Whang, H. S. & Lee, H. Electrochemical CO_2 reduction using alkaline membrane electrode assembly on various metal electrodes. *J. CO_2 Util.* **31**, 244-250 (2019).
48 Sankar, M. *et al.* Oxidation of glycerol to glycolate by using supported gold and palladium nanoparticles. *ChemSusChem* **2**, 1145-1151 (2009).
49 Villa, A. *et al.* Glycerol oxidation using gold-containing catalysts. *Acc. Chem. Res.* **48**, 1403-1412 (2015).
50 Birol, F. The future of hydrogen. Seizing today's opportunities. IEA. (2019).
51 Ruth, M. F., Mayyas, A. T. & Mann, M. K. Manufacturing Competitiveness Analysis for PEM and Alkaline Water Electrolysis Systems. (National Renewable Energy Lab.(NREL), Golden, CO (United States), 2019).
52 Kim, D. & Han, J. Comprehensive analysis of two catalytic processes to produce formic acid from carbon dioxide. *Appl. Energy* **264**, 114711 (2020).
53 Berg, L. & Yeh, A.-I. Dehydration of impure formic acid by extractive distillation. *US4735690A* (1988).
54 da Cunha, S., Rangaiah, G. & Hidajat, K. Design, optimization, and retrofit of the formic acid process II: Reactive distillation and reactive dividing-wall column retrofits. *Ind. Eng. Chem. Res.* **57**, 14665-14679 (2018).
55 Hua, X., Cao, R., Zhou, X. & Xu, Y. Integrated process for scalable bioproduction of glycolic acid from cell catalysis of ethylene glycol. *Bioresour. Technol.* **268**, 402-407 (2018).
56 Valderrama, M. A. M., van Putten, R.-J. & Gruter, G.-J. M. The potential of oxalic–and glycolic acid based polyesters (review). Towards CO_2 as a feedstock (Carbon Capture and Utilization–CCU). *Eur. Polym. J.* **119**, 445-468 (2019).